2014 IEEE Military Communications Conference

Detecting UWB Radar Signals with UWB Communication Interference

Hyunwoo Cho*, Yiyin Wang†, and Xiaoli Ma*

*School of Electrical and Computer Engineering, Georgia Institute of Technology, Atlanta, GA, 30332, USA
†Department of Automation, Shanghai Jiao Tong University, Shanghai, 200240, P. R. China

***Abstract*—Ultra wideband (UWB) technology has been widely researched for both radar and communication systems. However, detecting the presence of a signal is essential and challenging for many applications. In this paper, we propose a novel detector for UWB radar signals with UWB communication interference by exploiting the signal cyclic features. A single-cycle detector based on fundamental cyclic frequency of radar signal is proposed to detect UWB radar signal. Simulation results illustrate the possibility to detect the UWB radar signal under the coexistence of a UWB communication signal and the proposed scheme is compared with conventional detectors for UWB radar systems.**

I. Introduction

Ultra wideband (UWB) technology is widely researched for UWB communications and sensor applications. A feature of the UWB technology is low transmission power with ultra-short pulses at nanosecond scale duration [1]. Therefore, the UWB impulse radar can provide better performance in terms of high resolution ranging and penetrability compared to a narrow band radar. In addition, the UWB impulse radar can identify signatures of targets and robust to external narrow band interference [2]. Therefore, the UWB impulse radar can be suitable for various applications such as medicine care, human detection, through wall detection and surveillance systems in military [3]. Due to the limitation of the transmitted power and bandwidth for UWB technology, pulse compression technique has been proposed for achieving a reliable performance in target tracking and detection with employing matched filter [4]. However, an unknown shape of the reflected signal forbids processing of matched filter. Therefore, a blind detector based on correlation between received signals and delayed received signals has been proposed named as interleaved periodic correlation processing (IPCP) [5]. However, multiple thresholds are required for detecting multiple targets, because the threshold depends on the target size. In addition, setting multiple thresholds is also challenging, since increasing amount of IPCP output is difficult to estimate. In order to avoid multiple thresholds at IPCP detector, the parallel IPCP receiver has been proposed [6]. However, the structure of the parallel IPCP receiver is too complicated.

Since, both UWB radar and UWB communication systems employ monocycle Gaussian pulses [7], [8], energy detection based approaches such as the IPCP receiver cannot distinguish among them. Hence, detecting the UWB radar signals may be challenging under the UWB communication interference. In contrast, cyclostationarity-based detector can distinguish between UWB radar signal and UWB communication interference, because most of digital communication signals contain cyclostationarity and unique cyclic features. In addition, detectors based on cyclic features are robust to noise uncertainties. Therefore, it is widely used to detect signals of interest, such as primary user signals at cognitive radios. In addition, detecting wideband signal based on recovered cyclic spectrum using compressive sampling has been introduced [9]. Furthermore, detecting UWB signal from its cyclic feature under GMSK interference is recently introduced [10]. However, detecting UWB radar signal under UWB communication interference is yet discovered.

In this paper, we introduce the cyclic autocorrelation function (CAF) and the spectral correlation density function (SCD) of UWB radar signal from its autocorrelation function (AF). Since, both UWB radar and communication signals are real, we investigate the nonconjugate cyclostationarity to detect the UWB radar signal in the presence of UWB communication interference. Since, the UWB radar system contains pulse compression technique, it contains unique cyclic features from code sequences. Therefore, the UWB radar signals can be detected from its cyclic feature. In order to detect the UWB radar signals, we propose a single-cycle cyclostationarity-based detector in time domain based on fundamental cyclic frequencies. Consequently, the UWB radar signal can be detected from its cyclic feature, while its signal power is relatively small compared to the UWB communication interference.

The rest of this paper is organized as follows. Section II introduces the system model. Section III derives cyclostationarity of the UWB radar signal. Section IV introduces the cyclostationarity-based detector. Section V shows the numerical results, and Section VI concludes the paper.

II. System Model

At the UWB radar system, the transmitted signal after pulse integration with N monocycle Gaussian pulses $p(t)$ can be represented as follows [4]:

$$x(t) = \sum_{n=-\infty}^{\infty} \sum_{i=0}^{N-1} a_n c_i p(t - nT_r - iT_c), \qquad (1)$$

where $a_n \in \{\pm 1\}$ is the data sequence and T_r is signal repetition duration that $T_r = 1/\text{PRF}$, where PRF is the pulse repetition frequency. Each data sequence is modulated with

978-1-4799-6770-4/14 $31.00 © 2014 IEEE
DOI 10.1109/MILCOM.2014.141

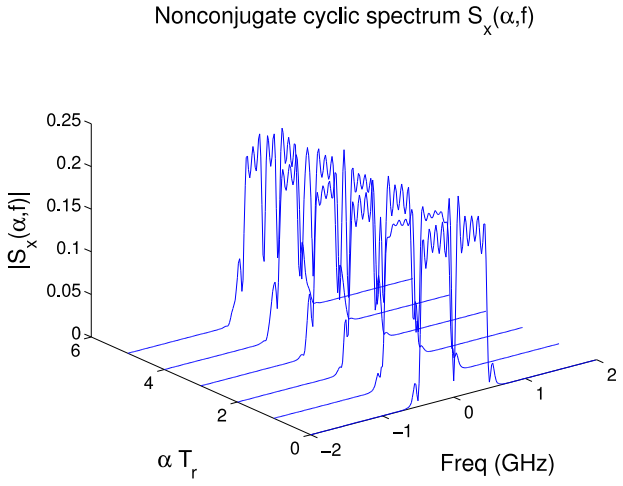

Fig. 1. The nonconjugate cyclic spectrum $S_x(\alpha, f)$ of a UWB radar signal with 11-Barker Codes.

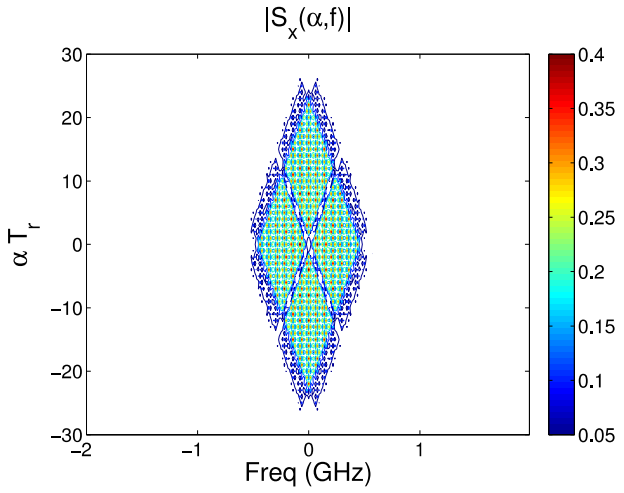

Fig. 2. Contour of $S_x(\alpha, f)$ of a UWB radar signal with 11-Barker Codes.

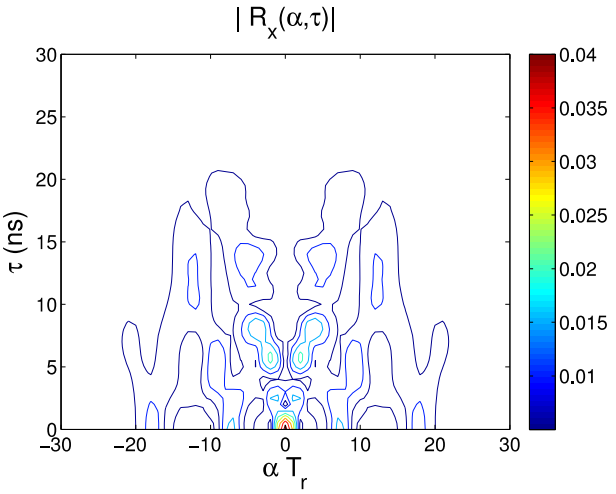

Fig. 3. Contour of $R_x(\alpha, f)$ of a UWB radar signal with 11-Barker Codes.

code sequences $c_i \in \{\pm 1\}$ and possible code sequences are introduced in [11]. Moreover, T_c is the chip duration, T_p is pulse duration, where $T_c > T_p$ and $T_r \gg NT_c$. Since, pulse integration with N pulses is deterministic, we can reorganize the signal $x(t)$ using the input-output filter relationship as follows:

$$x(t) = s(t) * c(t), \tag{2}$$

where $c(t) = \sum_{i=0}^{N-1} c_i \delta(t - iT_c)$ and $s(t) = \sum_{n=-\infty}^{\infty} a_n p(t - nT_r)$. In Eq. (2), the signal $x(t)$ can be viewed as the signal output of $s(t)$ passing through $c(t)$. Therefore the SCD is calculated as below [12]:

$$S_x(\alpha, x) = S_s(\alpha, f) C(f + \frac{\alpha}{2}) C^*(f - \frac{\alpha}{2}), \tag{3}$$

where $S_x(\alpha, f)$ and $S_s(\alpha, f)$ are the SCDs of the signal $x(t)$ and $s(t)$, respectively, and $C(f)$ is the Fourier transform of $c(t)$. In order to analyze the cyclic spectrum of $x(t)$, we first reshape the pulse function $p(t)$ in terms of its Fourier transform [13] as

$$p(t) = \int_{-\infty}^{\infty} P(\theta) e^{j2\pi\theta t} d\theta, \tag{4}$$

where $P(\theta)$ is the Fourier transform of $p(t)$.

III. Cyclostationarity

In this section, we investigate the cyclic spectrum of $x(t)$. The cyclostationarity can be extracted by the cyclic autocorrelation function (CAF) or the spectral-correlation density (SCD) function. The CAF of a signal $x(t)$ can be represented as follows [12]:

$$R_x^{\alpha}(\tau) = \lim_{T \to \infty} \frac{1}{T} \int_{-T/2}^{T/2} R_x(t, \tau) e^{-j2\pi\alpha t} dt, \tag{5}$$

where $R_x(t, \tau) = \mathrm{E}\{x(t + \tau/2) x^*(t - \tau/2)\}$ is the nonconjugate time-varying autocorrelation function (AF) which is periodic in time t, and α is the cyclic frequency with fundamental cycle $1/T_r$. Correspondingly, the conjugate AF is $R_{x^*}(t, \tau) = \mathrm{E}\{x(t + \tau/2) x(t - \tau/2)\}$. Therefore, the CAF and the SCD based on the nonconjugate AF are named as the nonconjugate CAF and SCD, respectively. As the UWB system emits real-value signal, the nonconjugate CAF and SCD are equal to the conjugate CAF and SCD. Therefore, we investigate the CAF and SCD of the UWB radar signal without specifying nonconjugate or conjugate in the following. The signal $x(t)$ exposes cyclostationarity, when there exists at least one non-zero α, satisfied $|R_x^{\alpha}(\tau)| > 0$. The SCD $S_x^{\alpha}(\tau)$ is defined as the Fourier transform of $R_x^{\alpha}(\tau)$ with respect to τ as

$$S_x^{\alpha}(f) = \int_{-\infty}^{\infty} R_x^{\alpha}(\tau) e^{-j2\pi f\tau} d\tau. \tag{6}$$

From Eq.(4), the AF of $x(t)$ can be represented as follows [13]:

$$R_x(t,\tau) = \int_{-\infty}^{\infty}\int_{-\infty}^{\infty} P(\theta)P^*(\phi)C(\theta)C^*(\phi)e^{j2\pi(\theta-\phi)t} \times e^{j2\pi(\theta+\phi)\tau/2}\sum_{n=-\infty}^{\infty}\sum_{m=-\infty}^{\infty}\mathrm{E}\{a_n a_m^*\} \times e^{-j2\pi\theta nT_r}e^{j2\pi\phi mT_r}d\theta d\phi \quad (7)$$

We assume that the data sequences a_n and a_m are uncorrelated, zero mean and wide-sense stationary. Therefore, the $\mathrm{E}\{a_n a_m^*\}$ is considered as the autocorrelation function of data sequence itself. As a result, we define $R_a(k) = \mathrm{E}\{a_n a_{n-k}^*\}$. Applying the Poisson sum formula $\sum_{n=-\infty}^{\infty} e^{-j2\pi nfT} = \frac{1}{T}\sum_{q=-\infty}^{\infty}\delta(f-\frac{q}{T})$, the AF of signal $x(t)$ can be simplified as follows:

$$\begin{aligned} R_x(t,\tau) &= \frac{1}{T_r}\int_{-\infty}^{\infty}\int_{-\infty}^{\infty} P(\theta)P^*(\phi)C(\theta)C^*(\phi)e^{j2\pi(\theta-\phi)t} \\ &\times e^{j2\pi(\theta+\phi)\tau/2}\sum_{k,l=-\infty}^{\infty} R_a(k)e^{-j2\pi\phi kT_r}\delta(\theta-\phi-\frac{l}{T_r})d\theta d\phi \\ &= \frac{1}{T_r}\sum_{l=-\infty}^{\infty} e^{-j2\pi t\frac{l}{T_r}}\int_{-\infty}^{\infty} P(\theta)P^*(\theta-\frac{l}{T_r})C(\theta)C^*(\theta-\frac{l}{T_r}) \\ &\times e^{j2\pi(\theta-\frac{l}{2T_r})\tau}\sum_{k=-\infty}^{\infty} R_a(k)e^{-j2\pi k(\theta-\frac{l}{T_r})T_r}d\theta \end{aligned} \quad (8)$$

From Eq.(8), $x(t)$ exposes wide-sense cyclostationarity with fundamental frequency of $1/T_r$. Since, $R_x(t,\tau)$ is already represented as a Fourier series form, the CAF of $x(t)$ can be easily derived as

$$\begin{aligned} R_x^{\alpha=\frac{l}{T_r}}(\tau) &= \frac{1}{T_r}\int_{-\infty}^{\infty} P(\theta)P^*(\theta-\frac{l}{T_r})C(\theta)C^*(\theta-\frac{l}{T_r}) \\ &\times e^{j2\pi(\theta-\frac{l}{2T_r})\tau}\sum_{k=-\infty}^{\infty} R_a(k)e^{-j2\pi k(\theta-\frac{l}{T_r})T_r}d\theta, \end{aligned} \quad (9)$$

and the SCD of $x(t)$ can be expressed as

$$\begin{aligned} S_x^{\alpha=\frac{l}{T_r}}(f) &= \frac{1}{T_r}P(f+\frac{l}{2T})P^*(f-\frac{l}{2T})C((f+\frac{l}{2T})T_c) \\ &\times C^*((f-\frac{l}{2T})T_c)S_a(2\pi(fT_r-\frac{l}{2})), \end{aligned} \quad (10)$$

where $S_a(f)$ is the power spectral density (PSD) of a_n. In Eqs. (9) and (10), the Fourier transform of code sequences $c(t)$ plays a role in determining unique cyclic features. Fig. 1 illustrates the details of the SCD of $x(t)$ with employing 11 Barker codes and 500 MHz bandwidth of the eighth-order Butterworth pulse as $p(t)$. It can be observed that $S_x(\alpha,f)$ contains multiple spectrum components at l/T_r, where $l \in 0,\pm1,\pm2,\cdots$. When $\alpha = 0$, $S_x(\alpha,f)$ is equal to PSD of the UWB radar signal.

IV. Cyclostationarity-based Detector under UWB communication interference

In this section, we focus on detecting the UWB radar signal based on its cyclostationarity. Under the UWB communication interference signal and noise signal, the received signal can be represented as follows:

$$\begin{aligned} y(t) &= \sum_{l=1}^{L}\beta_l x(t-\tau_l) + w(t) + i(t) \\ &= \sum_{n=-\infty}^{\infty}\sum_{l=1}^{L}\beta_l\sum_{i=0}^{N-1} a_n c_i p(t-nT_r-iT_c-\tau_l) + w(t) \\ &+ \sum_{m=-\infty}^{\infty}\sum_{u=0}^{N_f-1} d_m k_u p(t-mT_{sym}-uT_f), \end{aligned} \quad (11)$$

where $w(t)$ is the additive white Gaussian noise (AWGN) with zero mean and two-sided power spectral density $N_0/2$, $i(t)$ is UWB communication interference with employing same UWB pulse $p(t)$, T_{sym} is symbol duration for UWB communication interference, T_f is the frame duration, $d_m \in \{\pm1\}$ is information bit, and $k_u \in \{\pm1\}$ is the direct sequence (DS) codes. The important assumption is $T_r \neq T_{sym}$. Moreover, β_l is the power attenuation factor, τ_l is delay from lth target [4], and L is the total number of targets. In this paper, we assume that there is only one stationary target ($L = 1$) and $\beta = 1$. In order to reconstruct the cyclic spectrum with finite samples, we define a series of samples $\mathbf{y} = \{y[0], y[1], \cdots, y[N-1]\}$ with $y[k] = y(kT_s)$ for $k = 0, 1, \cdots, N-1$ and sampling frequency $f_s = 1/T_s \geq$ 2BW. Now, the CAF of $\mathbf{y}$ can be estimated as [9]

$$\hat{R}_y(a,\nu) = \left(\frac{1}{N}\sum_{n=0}^{N-1-\nu} r_{yy}(n,\nu)e^{-j\frac{2\pi}{N}an}\right)e^{-j\frac{\pi}{N}a\nu}, \quad (12)$$

where $r_{yy}(n,\nu) = \mathrm{E}\{x[n]x^*[n-\nu]\}$ is the discrete AF of $\mathbf{y}$ and $a \in [0, N-1]$ is the digital cyclic frequency which $\alpha = (a/N)f_s$. The SCD of $\mathbf{y}$ is represented as follows:

$$\hat{S}_y(a,b) = \frac{1}{N}\sum_{\nu=0}^{N-1}\hat{R}_y(a,\nu)e^{-j\frac{2\pi}{N}b\nu}, \quad (13)$$

where $\hat{S}_y(a,b)$ is the Fourier transform of the $\hat{R}_y(a,\nu)$ with respect to ν and $b \in [0, N-1]$ is the normalized digital frequency such that $f = (b/N)f_s$.

Since $w(t)$ is a stationary random process, $R_w^\alpha(\tau) = 0$ for all τ's, and $S_w^\alpha(f) = 0$ for all f's with $\alpha \neq 0$, where $R_w^\alpha(\tau)$ and $S_w^\alpha(f)$ are the CAF and SCD of noise signal, respectively. We assume the signal $x(t)$, $w(t)$ and $i(t)$ are mutually independent and the knowledge of T_r and T_{sym}. We define the set of cyclic frequency $\mathcal{A} = \{\alpha_l = \frac{l}{T_r}, l = \pm1, \pm2, \cdots, \pm K\}$, where $K = 2BT_r$ and B is the UWB radar signal bandwidth. From $T_r \neq T_{sym}$, the cyclic frequency of the UWB radar signal α_l leads $R_i^{\alpha_l}(\tau), S_i^{\alpha_l}(f) \approx 0$, when $\mathcal{A} \notin \{\alpha_k = \frac{k}{T_{sym}}, k = \pm1, \pm2, \cdots\}$, where $R_i^{\alpha_l}(\tau)$ and $S_i^{\alpha_l}(f)$ are the CAF and SCD of UWB communication interference, respectively.

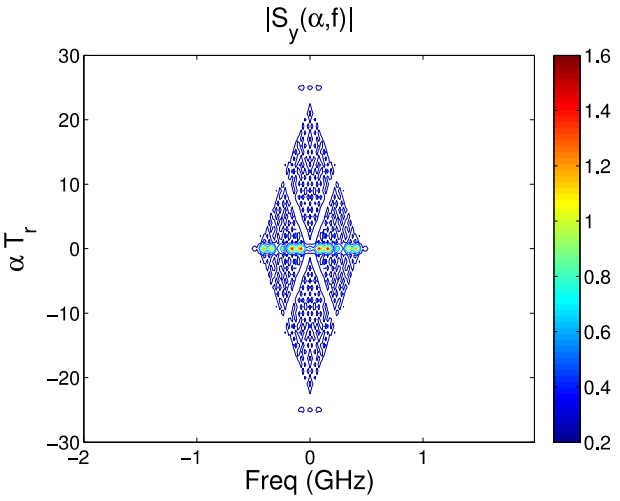

Fig. 4. Contour of $S_y(\alpha, f)$ under the UWB communication interference with SIR $= -6$ dB

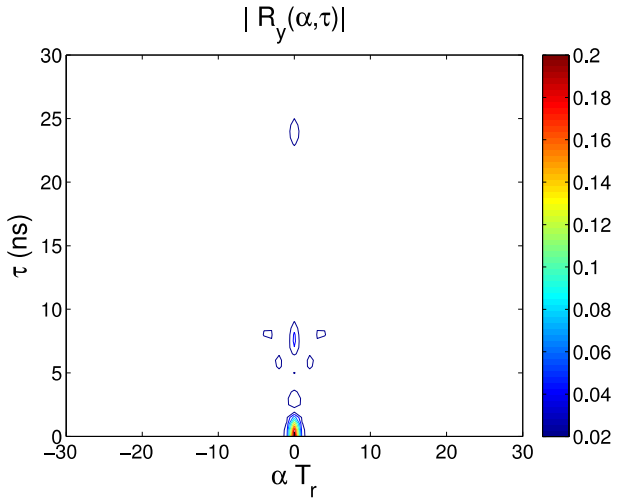

Fig. 5. Contour of $R_y(\alpha, \tau)$ under the UWB communication interference with SIR $= -6$ dB

After vectorizing $\hat{r}_y(a, \nu) = \text{vec}\{\hat{R}_y(a, \nu)\}$ and stacking $\hat{r}_y(a, \nu)$ into a vector $\hat{\mathbf{c}}$, the binary hypotheses test can be represented as:

$$\begin{aligned} \mathcal{H}_0 &: \hat{\mathbf{c}} = \epsilon \\ \mathcal{H}_1 &: \hat{\mathbf{c}} = \mathbf{c} + \epsilon, \end{aligned} \tag{14}$$

where $\mathbf{c}$ is the non-random true vector of the CAF values, ϵ is the estimation error that is asymptotically zero-mean Gaussian distributed, $\mathcal{H}_0$ is represented the absence of the UWB radar signal and $\mathcal{H}_1$ shows the presence of the UWB radar signal.Therefore, asymptotic normality of $\mathbf{c}_n$ leads to the test statistics as follows [9]:

$$\mathcal{T} = K(\mathbf{c})^H(\hat{\mathbf{\Sigma}})^{-1}\mathbf{c}, \tag{15}$$

where $\hat{\mathbf{\Sigma}}$ is the estimated covariance matrix following from [9]. The fact that $\mathcal{T}$ under $\mathcal{H}_0$ converges to $\mathcal{X}^2$ distribution with $2K$ degrees of freedom and normal distribution [14] leads to a constant false alarm rate (CFAR) test. Therefore, for a given probability of false alarms $P_f = Pr\{\mathcal{T} \geq \Gamma|\mathcal{H}_0\}$, a threshold Γ can be determined from the table of a central $\mathcal{X}^2$ distribution, and then the detection probability can be evaluated as $P_d = Pr\{T \geq \Gamma|\mathcal{H}_1\}$.

V. Numerical Result

In this section, we introduce the simulation results of cyclostationarity-based detector under the UWB communication interference and noise. The system parameters for simulation are as follows. For both the UWB radar and the UWB communication signals, 500 MHz bandwidth of the eighth-order Butterworth pulse is employed in [10] and the sampling frequency is 2 GHz. In order to transmit a radar signal, the UWB radar adopts 11-Barker codes for pulse integration. The signal repetition frequency (PRF) is 20 MHz, such that signal with 11-Barker codes is emitted at every $T_r = 50$ ns. Therefore, the fundamental cycle frequency is $1/T_r = 20$ MHz. Other parameters are set as $T_c = 2$ ns and $N_c = 11$. Otherwise, the symbol period for the UWB communication interference $T_{sym} = 32$ ns with a frame duration $T_f = 8$ ns and $N_f = 4$. The total length of observed time is 10 μs. Figs. 2 and 3 illustrate contours of the nonconjugate SCD and CAF of the UWB radar signal itself $s(t)$, respectively. Since the UWB radar system employs pulse integration, the SCD and CAF have unique cyclic features and this can be useful to distinguish from unknown interferences. Figs. 4 and 5 illustrate the contours of the SCD and CAF in the presence of the UWB communication interference. In these figures, we ignore the noise and fixed the signal to interference ratio (SIR) that is the ratio of the UWB radar signal power to the UWB communication power as -6 dB. We can easily compare the features of the SCD and CAF. While the SCD remains similar shape compared to Fig. 2, the CAF loses lots of components compared to Fig. 3, because relatively strong UWB communication interference may prohibit cyclic features of UWB radar signal at time domain. In order to estimate the SCD and CAF of the UWB radar signal, the received signal is segmented by L blocks, where block length is defined as $2T_r$. Therefore, the number of samples per block is $N = 200$ and the AF can be calculated as follows:

$$\hat{r}_{yy} = \frac{1}{L}\sum_{k=0}^{L-1}\mathbf{y}(k)\mathbf{y}^H(k), \tag{16}$$

where $\mathbf{y}(k)$ is the kth signal segment sample vector. Therefore, we can estimate the CAF and the SCD by plugging (16) into Eqs. (12) and (13).

Fig. 6 illustrates the probability of detection versus signal to noise ratio (SNR) with different SIR and compare to the conventional IPCP detectors [5], where SNR is defined as the power ratio between the UWB radar signal power and noise power. We also assume that we do not have any knowledge about the statistics of UWB communication

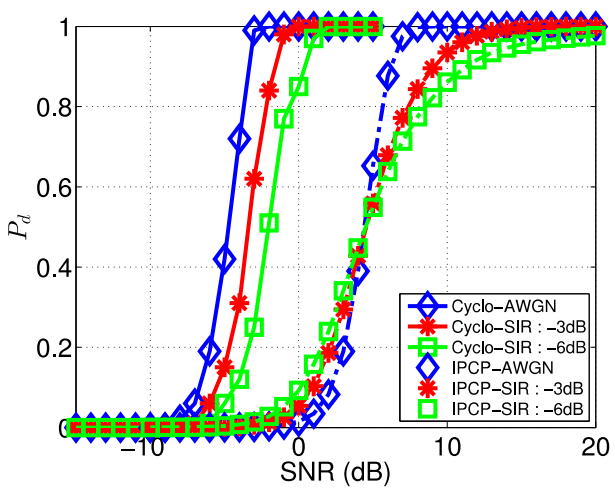

Fig. 6. Detection probability of UWB radar signal

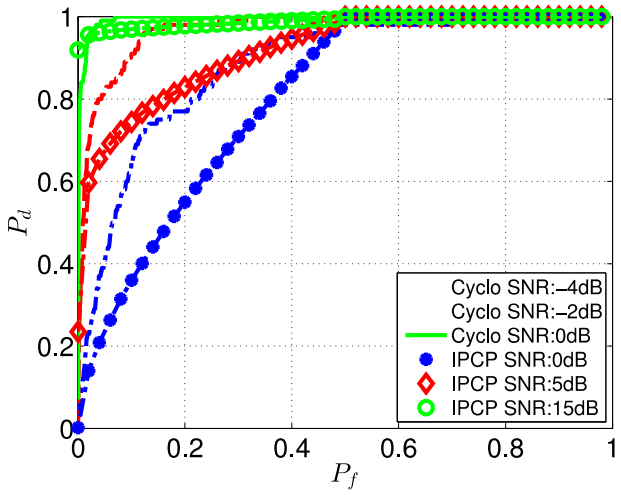

Fig. 7. Receiver Operation Characteristic with SIR $= -6$ dB

interference. Moreover, the probabilities of false and detection for IPCP detector are assumed as Gaussian distribution [5]. According to Fig. 6, cyclostationarity-based detectors show better performance regardless of interference. Without UWB communication interference, our proposed detector achieves around 10 dB gain at $P_d = 1$. In addition, in the presence of UWB communication interference with SIR $= -6$ dB, our proposed detector has around 20 dB gain at $P_d = 1$.

Since the CFAR test can be applied to determine the receiver operating characteristics (ROC), Fig. 7 shows ROC that illustrates P_d versus P_f with SIR $= -6$ dB among various SNR values. It shows that our proposed detectors can maintain P_d larger than 0.9 at 0 dB SNR and the IPCP detectors can achieve P_d greater than 0.9 with SNR $= 15$ dB. Therefore, the SNR gap between the IPCP detectors is around 15 dB. Although the IPCP detectors with SNR $= 5$ dB show better performance compared to our proposed detector with SNR $= -4$ dB, there is still 9 dB SNR gap between them.

VI. Conclusion

In this paper, we proposed the UWB radar detector based on its cyclic feature under UWB communication interference and noise. We first explore the cyclic autocorrelation function and spectral correlation density of the UWB radar signal. Based on the unique cyclic features of the UWB radar signal, we can distinguish the radar signal and the UWB communication interference. As a result, cyclostationarity-based detector is robust to interference and noise signal. Through simulations, our proposed detector can detect the UWB radar signal under the UWB communication interference at low SIR and show better performance compared to the conventional IPCP detector.

Acknowledgement

Part of this work is supported by the Georgia Tech Ultrawideband Center of Excellence (http://www.uwbtech.gatech.edu/).

References

[1] M. Z. Win and R. A. Scholtz, "Impulse radio: how it works," *IEEE Commun. Lett.*, vol. 2, no. 2, pp. 36–38, Feb. 1998.

[2] I. Immoreev and P. Fedotov, "Ultra wideband radar systems: advantages and disadvantages," in *Proc. IEEE Conference on Ultra Wideband Systems and Technologies, Digest of Papers*, Baltimore, MD, May. 2002, pp. 201–205.

[3] J. D. Taylor, Ed., *Ultra-wideband Radar Technology*. CRC Press, 2000.

[4] M. Hussain, "Ultra-wideband impulse radar-an overview of the principles," *IEEE Aerosp. Electron. Syst. Mag.*, vol. 13, no. 9, pp. 9–14, Sep. 1998.

[5] I. Immoreev and P. Fedotov, "Detection of UWB signals reflected from complex targets," in *Proc. IEEE Conference on Ultra Wideband Systems and Technologies, Digest of Papers*, Baltimore, MD, May. 2002, pp. 193–196.

[6] H. Hatano, H. Okada, T. Yamazato, and M. Katayama, "Performance analysis of UWB impulse radar using parallel IPCP receiver," in *Proc. 1st International Symp. on Wireless Communication Systems*, MAURITIUS, Sept. 2004, pp. 115–119.

[7] J. Dederer, B. Schleicher, F. De Andrade Tabarani Santos, A. Trasser, and H. Schumacher, "FCC compliant 3.1-10.6 GHz UWB pulse radar system using correlation detection," in *Proc. IEEE/MTT-S International Microwave Symposium*, Honolulu, HI, June. 2007, pp. 1471–1474.

[8] L. Yang and G. Giannakis, "Ultra-wideband communications: an idea whose time has come," *IEEE Signal Process. Mag.*, vol. 21, no. 6, pp. 26–54, Nov. 2004.

[9] Z. Tian, Y. Tafesse, and B. Sadler, "Cyclic feature detection with sub-Nyquist sampling for wideband spectrum sensing," *IEEE J. Sel. Topics Signal Process.*, vol. 6, no. 1, pp. 58–69, Feb. 2012.

[10] Y. Wang, X. Ma, and Q. Zhou, "Detecting UWB signals using cyclic features," in *Proc. IEEE International Conference on Ultra-Wideband (ICUWB)*, Sydney, NSW, Sept. 2013, pp. 142–147.

[11] M. Hussain, "Principles of high-resolution radar based on nonsinusoidal waves. I. signal representation and pulse compression," *IEEE Trans. Electromagn. Compat.*, vol. 31, no. 4, pp. 359–368, Nov. 1989.

[12] W. Gardner, "Exploitation of spectral redundancy in cyclostationary signals," *IEEE Signal Process. Mag.*, vol. 8, no. 2, pp. 14–36, Apr. 1991.

[13] M. Öner, "On the cyclostationary statistics of ultra-wideband signals in the presence of timing and frequency jitter," *AEU-International Journal of Electronics and Communications*, vol. 62, no. 3, pp. 174–184, Mar. 2008.

[14] A. Dandawate and G. Giannakis, "Statistical tests for presence of cyclostationarity," *IEEE Trans. Signal Process.*, vol. 42, no. 9, pp. 2355–2369, Sep. 1994.